

## Single-Crystal X-ray Diffraction and Solution Studies of Anion– $\pi$ Interactions in *N*-(Pentafluorobenzyl)pyridinium Salts

Michael Giese,<sup>[a]</sup> Markus Albrecht,\*<sup>[a]</sup> Tatjana Repenko,<sup>[a]</sup> Johannes Sackmann,<sup>[a]</sup> Arto Valkonen,<sup>[b]</sup> and Kari Rissanen\*<sup>[b]</sup>

**Keywords:** Anion– $\pi$  interactions / Pyridinium salts / Triiodides / Noncovalent interactions / Structure elucidation

A solid-state structural study on anion– $\pi$  interaction in various *N*-(pentafluorobenzyl)pyridinium salts accompanied by NMR spectroscopic investigations is presented. The crystal structures of **1a–1d** reveal different kinds of contacts with anions, including anion– $\pi$  interactions. In particular, the

solid-state structure of **1b**–I<sub>3</sub> shows distinct evidence of anion– $\pi$  interactions. Attempts to study anion– $\pi$  interactions in solution were not successful, but their presence in solution could not be ruled out.

### Introduction

Anions play a crucial role in biological and chemical systems.<sup>[1]</sup> A large number of enzymes and enzymatic cofactors are negatively charged,<sup>[2]</sup> and diseases such as cystic fibrosis are caused by a malfunction of anion channels.<sup>[3]</sup> This shows the high relevance of selective anion receptors. Common anion receptors are based on electrostatic attractions, hydrogen bonds, or hydrophobic effects.<sup>[4]</sup>

In recent years, a new type of noncovalent interaction has gained considerable attention in the field of anion recognition, namely, the anion– $\pi$  interaction.<sup>[5]</sup> In the 1990s, Schneider et al.<sup>[6]</sup> reported the first experimental evidence for the attractive interaction of the negatively charged parts of a molecule with polarized  $\pi$ -systems. Following the computational studies of Mascial, Alkorta and Deyà<sup>[7a,7b]</sup> supported the attractive nature and explained it with the interaction of an anion with the  $\pi$ -system of an electron-deficient arene. This intermolecular force is suggested to be appropriate for the design of superior anion receptors and, therefore, the interest in anion– $\pi$  interactions has grown rapidly within the last 20 years.<sup>[5]</sup>

Since the report by Schneider et al.,<sup>[6]</sup> numerous theoretical and structural studies have been performed to show the relevance of anion– $\pi$  interactions.<sup>[7]</sup> In contrast, the role of this noncovalent interaction in solution has remained an

open question.<sup>[8]</sup> In 2008, we started our work on anion– $\pi$  interactions in (pentafluorophenyl)ammonium and -phosphonium salts.<sup>[9]</sup> Our first crystallographic results revealed a versatile positional variation of the anion above the C<sub>6</sub>F<sub>5</sub> unit. To describe the observed binding motifs, the hapticity ( $\eta$ ) nomenclature for cation– $\pi$  interactions was transferred to systems with anion– $\pi$  interactions. Further investigations showed that the position of the anion above an electron-deficient arene can be controlled by directing substituents in the molecular skeleton through the utilization of CH–anion and NH–anion interactions.<sup>[10]</sup> Moreover, the effect of the electron density of the  $\pi$ -system on the interaction with anions was extensively studied. The attraction in highly fluorinated systems (four to five fluorine atoms) is switched to repulsion in arenes with a low degree of fluorination (two to three fluorine atoms).<sup>[11]</sup> Crystallographic studies on the role of the anions in anion– $\pi$  interactions do not show dependence on the geometry of the anion.<sup>[12]</sup> However, serendipity led to the remarkable stabilization of the labile tetraiodide dianion (I<sub>4</sub><sup>2-</sup>) by anion– $\pi$  interactions.<sup>[13]</sup> Our first attempts to clarify the relevance of anion– $\pi$  interactions in solution by studying (pentafluorobenzyl)phosphonium salts did not show any evidence for this intermolecular force in chloroform.<sup>[14]</sup>

The present study reports the experimental evidence of anion– $\pi$  interactions in crystals of *N*-(pentafluorobenzyl)pyridinium salts. Additional solution NMR spectroscopic investigations have been performed.

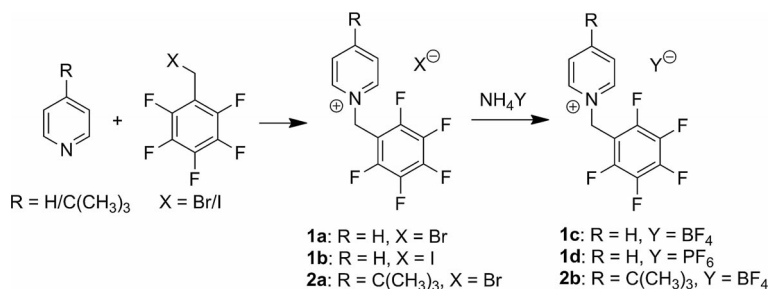
### Results and Discussion

On the basis of previous results on the directing effects of substituents on the position of anions above electron-poor arenes, a series of *N*-(pentafluorobenzyl)pyridinium salts (Br, I, PF<sub>6</sub>, and BF<sub>4</sub>) was synthesized. In these salts,

[a] Institut für Organische Chemie, RWTH Aachen, Landoltweg 1, 52074 Aachen, Germany  
E-mail: markus.albrecht@oc.rwth-aachen.de  
<http://www.oc.rwth-aachen.de/akalbrecht/>

[b] Department of Chemistry, Nanoscience Center, University of Jyväskylä, Survontie 9, 40014 Jyväskylä, Finland  
E-mail: kari.t.rissanen@jyu.fi  
<https://www.jyu.fi/kemia/tutkimus/orgaaninen/en/research/rissanen>

Supporting information for this article is available on the WWW under <http://dx.doi.org/10.1002/ejoc.201301336>.



Scheme 1. Synthesis of the *N*-(pentafluorobenzyl)pyridinium salts.

the anion should be located above the  $\pi$ -system by fixation through CH–anion interactions of the pyridinium moiety or encapsulated in a cradle of anion– $\pi$  interactions with both electron-deficient arenes (see Scheme 1). A series of solid-state structures could be obtained and showed anion– $\pi$  as well as CH–anion interactions. Additionally, NMR titration experiments with *n*-tetrabutylammonium salts were performed to investigate the interplay of the interactions in solution.

### Synthesis of Pyridinium Compounds

The *N*-(pentafluorobenzyl)pyridinium halides **1a**, **1b**, and **2a** were prepared by a nucleophilic substitution of pyridine or 4-*tert*-butylpyridine with the corresponding pentafluorobenzyl halide. By serendipity, the iodide was oxidized in air during the crystallization, and the triiodide salt of the *N*-(pentafluorobenzyl)pyridinium compound (**1b**-I<sub>3</sub>) was obtained. The tetrafluoroborate (**1c** and **2b**) and hexafluorophosphate (**1d**) salts were obtained by salt metathesis from saturated aqueous solutions.

All compounds – except **1b**-I<sub>3</sub> – were fully characterized by standard analytical methods, and representative solid-state structures were obtained.

### Solid-State Studies

Owing to the complexity of the interplay of noncovalent interactions in the crystal lattice, the overall packing will not be described. The focus will be on the relevant interactions of adjacent ions. Relevant anion– $\pi$  contacts and arene–arene interactions will be discussed in detail. It should be noted that the crystal structures of the non-fluorinated analogues of the compounds described in the following are well known.<sup>[15]</sup> However, these structures show exclusively CH–anion interactions and give no hint of anion– $\pi$  interactions with neither the phenyl nor the pyridinium unit.

#### *N*-(Pentafluorobenzyl)pyridinium Bromide and Iodide (**1a** and **1b**)

Crystals of **1a**·H<sub>2</sub>O were obtained by the diffusion of ethyl acetate into a solution of **1a** in dimethyl sulfoxide (DMSO). The cocrystallized water molecule networks the anions to form a zigzag strand [Figure 1c; O···Br 3.401(2), 3.503(2) Å]. This strand is bordered by electron-deficient

arenes (pentafluorophenyl and pyridinium units). The bromide anion is in close contact with the pentafluorophenyl group [C<sup>1–3</sup>···Br 3.922(3), 3.478(3), 3.726(3) Å;  $\eta^3$ -type] and the pyridinium unit [C<sup>2,5,6</sup>···Br 3.951(3), 3.824(3), 3.662(3) Å, N<sup>1</sup>···Br 3.750(2) Å;  $\eta^4$ -type]. However, the shortest anion– $\pi$  contact was found with the pyridinium unit of an *N*-(pentafluorobenzyl)pyridinium cation averted from the zigzag strand [C<sup>5</sup>···Br 3.395(3) Å, N<sup>1</sup>···Br 3.803(2) Å;  $\eta^2$ -type]. Additional CH–anion interactions were found between the benzyl protons and neighboring bromide anions [CH···Br 2.985 Å; *x*, *y* – 1, *z* symmetry operation].

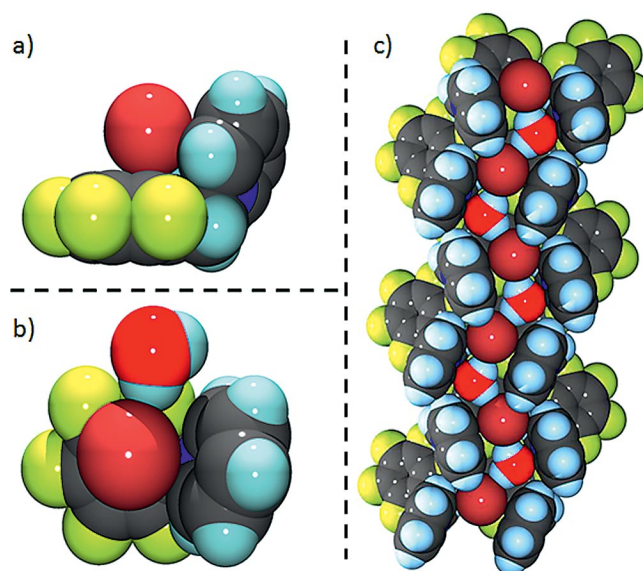


Figure 1. (a) Side and (b) top views of the asymmetric unit in the crystal structure of **1a**·H<sub>2</sub>O illustrating the close contact between the anions and cations; (c) view of the molecular packing; black: carbon, white: hydrogen, green: fluorine, blue: nitrogen, red: oxygen, dark red: bromine.

A closely related structure is observed for **1b**, which crystallizes in the triclinic space group  $P\bar{1}$  and shows two anions and two cations per asymmetric unit (Figure 2). The selected anion–cation pairs (**1b**-A and **1b**-B) possess similar structural features, and both anions show short CH–anion distances [CH···I: **1b**-A: 2.920, 2.946, 3.068 Å (all from neighboring cations), **1b**-B: 2.907, 3.025 Å (latter from

neighboring cation of A)] as well as close anion- $\pi$  contacts to the pentafluorophenyl unit [**1b**-A: C<sup>5</sup>-6...I 4.005(3), 3.852(3) Å, C<sup>2</sup>-4...I 3.802(3), 3.629(3), 4.081(3) Å to I of B; **1b**-B: C<sup>2</sup>...I 3.953(3) Å]. The crystal packing reveals the T-stacking of the pentafluorophenyl moieties of neighboring cations (CF...aryl 3.259 Å; see Figure S1). There is a symmetry-related  $\pi$ ... $\pi$  stacking interaction between the pyridinium rings of adjacent cations of A with a shortest C...C distance of 3.374(4) Å [center...center 3.60 Å;  $-x + 2, -y, -z$  symmetry operation].

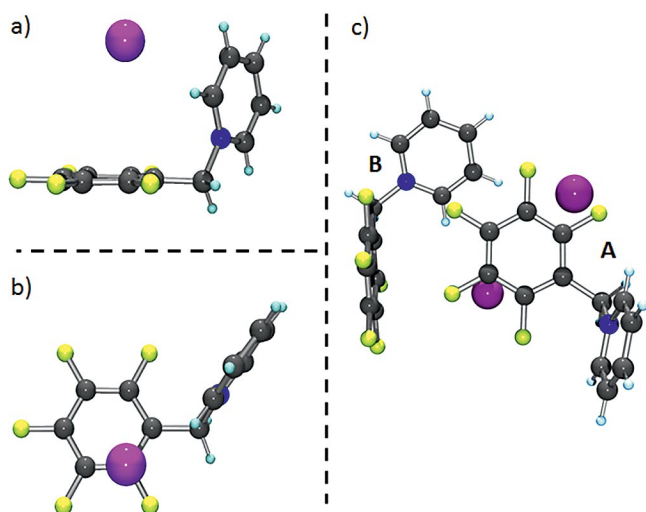


Figure 2. (a and b) Two views of the selected anion-cation pair of **1b**-A and (c) the asymmetric unit of **1b** showing the assignment of the ion pairs; black: carbon, white: hydrogen, green: fluorine, blue: nitrogen, violet: iodine.

### *N*-(Pentafluorobenzyl)pyridinium Tetrafluoroborate and Hexafluorophosphate (**1c** and **1d**)

The crystal structure of **1c** shows obvious similarities to that of **1b**. Like **1b**, compound **1c** crystallizes in the triclinic space group  $P\bar{1}$  with two anions and two cations per asymmetric unit (Figure 3). In the selected anion-cation pairs, both anions are fixed by CH-anion interactions [C-H...F: **1c**-A: 2.582, 2.620 Å; **1c**-B: 2.504 Å] above the  $\pi$ -system [C<sup>2</sup>-3...F: **1c**-A: 3.066(3), 3.205(3) Å, **1c**-B: 2.996(3), 3.331(3) Å; C<sub>GAr</sub>...F: **1c**-A: 3.34 Å, **1c**-B: 3.65 Å; C<sub>G</sub> is the centroid of the aryl ring] and show  $\eta^2$ -type anion- $\pi$  contacts. Anion- $\pi$   $\eta^2$ -type interactions from the anion of B to the pyridinium moiety of the adjacent A pair were also observed in the structure of **1c** [N...F 3.103(3) Å, C<sup>6</sup>...F 3.080(3) Å;  $-x + 1, -y + 1, -z + 2$  symmetry operation]. Additional CH-anion interactions with the benzyl protons [**1c**-A: C-H...F 2.469, 2.395 Å; **1c**-B: C-H...F 2.259, 2.293 Å] are present in the solid-state structure, and almost all pyridyl protons show very weak CH-anion contacts [C-H...F 2.400–2.564 Å].

Crystals of **1d** were obtained by diffusion of diethyl ether into a solution of **1d** in *N,N*-dimethylformamide (DMF). The salt crystallizes in the orthorhombic space group  $Pbca$ . In contrast to the previously described structures, **1d** shows

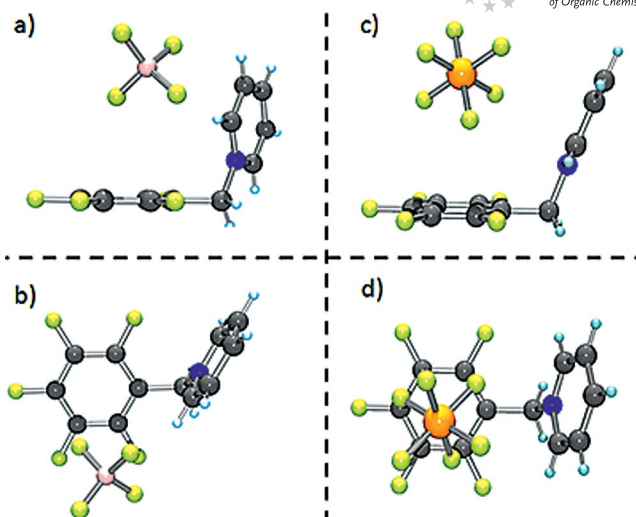


Figure 3. (a and c) Side and (b and d) top views of the solid-state structures of **1c** (selected **1c**-A pair) and **1d**; black: carbon, white: hydrogen, green: fluorine, blue: nitrogen, orange: phosphorus, pink: boron.

simultaneous anion- $\pi$  interactions, whereby both electron-deficient arenes face the hexafluorophosphate anion in parallel. The C<sub>6</sub>F<sub>5</sub> and C<sub>5</sub>H<sub>5</sub>N rings span ( $\angle$ C<sub>6</sub>F<sub>5</sub>-C<sub>6</sub>H<sub>5</sub>N 65.93°) an electron-deficient cradle for the hexafluorophosphate ion that leads to attractive anion- $\pi$  interactions [C<sub>6</sub>F<sub>5</sub>: C...F 2.823(3)–3.563(3) Å, C<sub>GAr</sub>...F 3.27 Å; C<sub>5</sub>H<sub>4</sub>N: C...F 3.152(3)–3.461(3) Å]. The anion is slightly shifted away from the centers of the  $\pi$ -systems. A wider view of the crystal packing shows that there are additional anion- $\pi$  contacts with the pyridinium unit of an adjacent cation [C/N...F 3.065(2)–3.717(3) Å] and several CH-anion interactions [C-H...F 2.445–2.649 Å].

All relevant anion- $\pi$  distances of the previously described structures are summarized in Table S2.

As already mentioned in the introduction, an additional *N*-(pentafluorobenzyl)pyridinium salt structure was found. The triiodide **1b**-I<sub>3</sub> was obtained by crystallization of **1b** in methanol under an oxidative atmosphere. It crystallized in the triclinic space group  $P\bar{1}$  with two halves of a triiodide ion in the asymmetric unit (central iodine atoms in special positions) and shows a remarkable feature (Figure 4). The crystal structure reveals that two *N*-(pentafluorobenzyl)pyridinium cations create an electron-deficient box around one triiodide anion. This leads to close contacts between the central iodine atom and the pentafluorophenyl [C...I 3.765(4)–4.003(4) Å; C<sub>GAr</sub>...I 3.63 Å] ring as well as to the pyridinium units [C/N...I 3.858(4)–4.106(5) Å; C<sub>GAr</sub>...I 3.74 Å]. The second triiodide anion shows anion- $\pi$  contacts between the terminal iodine atoms and the pyridinium unit [C/N...I 3.657(3)–4.196(4) Å, C<sub>GAr</sub>...I 3.69 Å;  $-x + 1, -y, -z + 1$  symmetry operation]. Additionally, interactions between the central [C<sup>2</sup>-3...I 3.885(4), 4.003(4) Å, C<sub>GAr</sub>...I 4.32 Å;  $\eta^2$ -type] and terminal iodine atoms [C<sup>1,6</sup>...I 3.608(4), 3.910(4) Å] with the pentafluorophenyl groups are observed. No CH...I contacts were found in the structure of **1b**-I<sub>3</sub>.

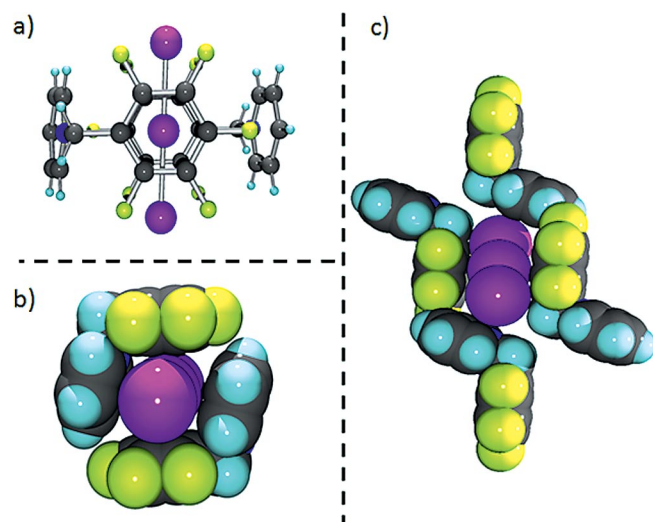


Figure 4. (a and b) Two different views of the encapsulated triiodide anion in the solid-state structure of **1b**-I<sub>3</sub> and (c) the second triiodide anion in the unit cell; black: carbon, white: hydrogen, green: fluorine, blue: nitrogen, violet: iodine.

The presented series of *N*-(pentafluorobenzyl)pyridinium salts demonstrate the interactions between bromide, iodide, tetrafluoroborate, and hexafluorophosphate anions and electron-deficient pentafluorobenzyl and pyridinium units. The strongest structural evidence for the attractive nature of anion- $\pi$  interactions within this series is found in the solid-state structure of **1b**-I<sub>3</sub>. The C<sub>6</sub>F<sub>5</sub> unit and the C<sub>5</sub>NH<sub>5</sub> moiety show short distances to the linear I<sub>3</sub><sup>-</sup> anion. Structural hints of anion- $\pi$  interactions in the solid state are numerous,<sup>[7]</sup> but their role in solution remains an open question.<sup>[5]</sup>

### Solution Studies

As already mentioned in the introduction, several attempts have been made to investigate the relevance of anion- $\pi$  interaction in solution.<sup>[8,14]</sup> However, irrefutable evidence is still missing. Competing noncovalent interactions and solvation effects make it difficult to obtain distinct evidence for anion- $\pi$  interactions in solution.

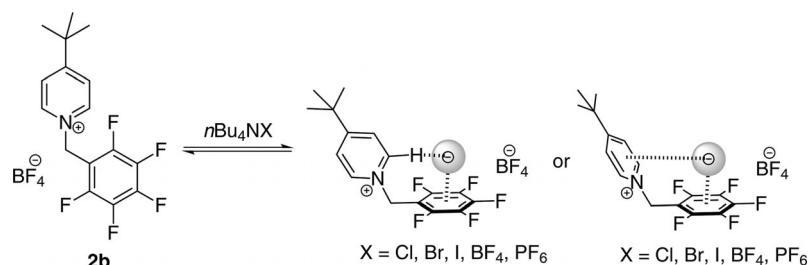
Earlier studies with (pentafluorobenzyl)phosphonium salts showed that CH-anion interactions cover the attraction between anions and electron-deficient  $\pi$ -systems. In the present study, *N*-(pentafluorobenzyl)pyridinium salts were

used owing to the lower acidity of their protons and their higher air stability. Owing to the low solubility of *N*-(pentafluorobenzyl)pyridinium tetrafluoroborate as well as hexafluorophosphate in chloroform, the corresponding 4-*tert*-butylpyridinium salts were synthesized. Only the tetrafluoroborate **2b** showed an appropriate solubility in chloroform for NMR spectroscopic measurements. To determine the differential binding constants for the 4-*tert*-butyl-*N*-(pentafluorobenzyl)pyridinium cation, **2b** was titrated with tetrabutylammonium chloride, bromide, iodide, tetrafluoroborate, and hexafluorophosphate. The investigated solution studies are summarized in Scheme 2.

Initial studies on the stoichiometry of the investigated anion-receptor complexes (guest: receptor) by the method of Job<sup>[16]</sup> revealed significant shifts for the benzyl and pyridyl protons in the <sup>1</sup>H NMR spectra and for the *ortho*-, *meta*-, and *para*-fluorine atoms in the <sup>19</sup>F NMR spectra (Figure 5). Interestingly, the stoichiometry of the complexes varies in dependence of the signal monitored in the NMR spectra. Although the titrations with tetrabutylammonium tetrafluoroborate and hexafluorophosphate do not show systematic development during the measurement, the stoichiometry for the halides can be determined. The benzyl and *ortho*-fluorine signals show 1:1 complexes for all three halides. The pyridyl proton signal reveals a 1:1 complex for the chloride and bromide and a 1:2 stoichiometry for the iodide. The *meta* and *para* <sup>19</sup>F signals show a 2:1 complex for the chloride and a 1:1 complex for the iodide. The data for the bromide titration does not show a systematic behavior. However, the differences in the complex stoichiometries might be attributed to the rather flat Job curves and should not be overemphasized (see Table S3).

To ascertain the differential association constants, a 0.1 M stock solution of **2b** and a 0.4 M solution of the tetrabutylammonium salts were prepared. The solutions were mixed in different ratios and filled to a standard volume of 0.7 mL to guarantee a fixed receptor concentration.

The signals of the pyridyl protons in the NMR spectra used to produce the titration curves show a downfield shift upon the addition of halides and an upfield shift with tetrafluoroborate and hexafluorophosphate anions. Furthermore, the shifts for the halides are significantly stronger than for the less-coordinating anions. A comparison of the different signals followed during the NMR spectroscopic measurements shows that there is a strong upfield shift for the *ortho*-fluorine signal, whereas the signals of the benzyl and pyridyl protons as well as that of the *para*-fluorine



Scheme 2. Investigated equilibrium in solution.

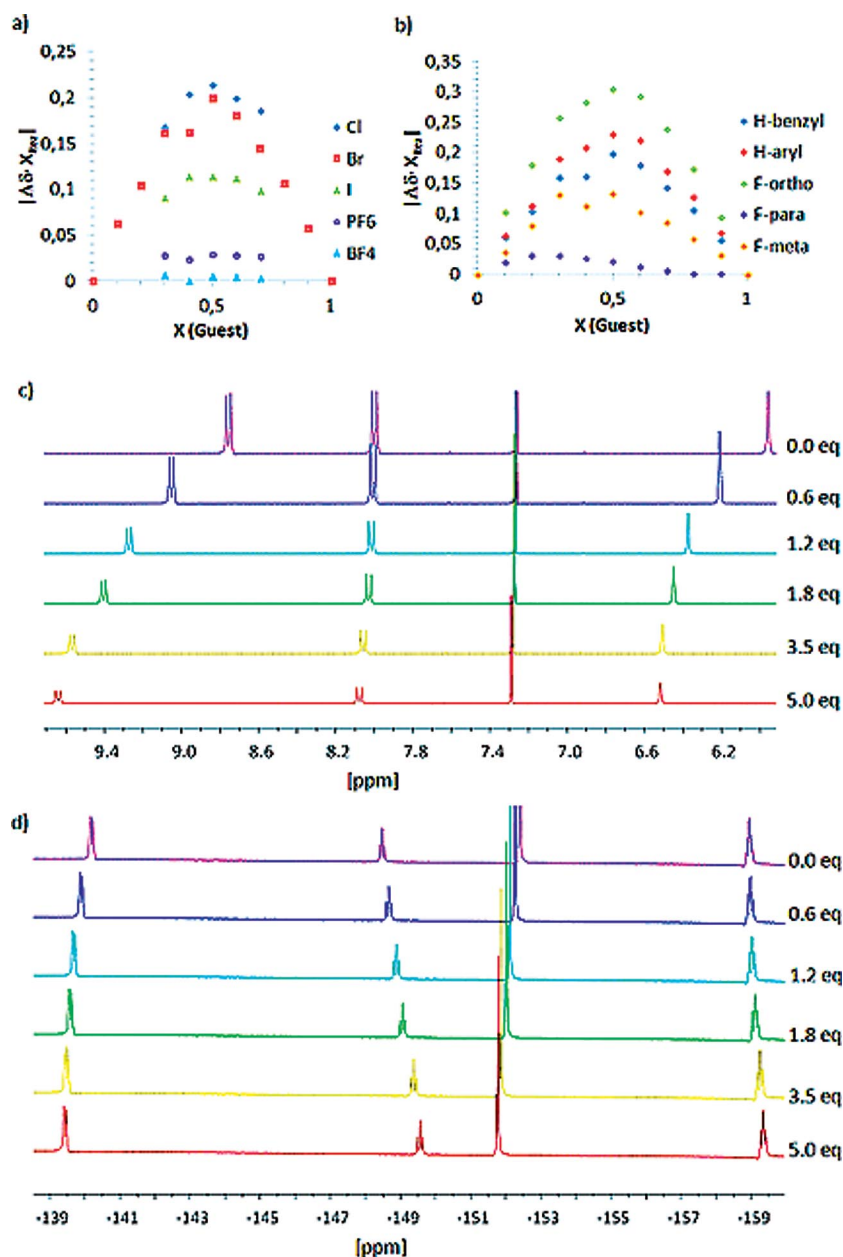


Figure 5. (a) Job plots for the pyridinium complexes with various anions (Cl, Br, I, PF<sub>6</sub>, and BF<sub>4</sub> added as tetrabutylammonium salt). (b) Job plots for the titration of **2b** with *n*Bu<sub>4</sub>NBr in CDCl<sub>3</sub>. (c) Selected <sup>1</sup>H NMR spectra for the titration of **2b** with *n*Bu<sub>4</sub>NBr in CDCl<sub>3</sub>. (d) Selected <sup>19</sup>F NMR spectra for the titration of **2b** with *n*Bu<sub>4</sub>NBr in CDCl<sub>3</sub>.

atom shift downfield. For the *meta*-fluorine signal, a systematic shift could not be observed. The determined binding constants under consideration of the complex stoichiometries are summarized in Table 1.

Table 1. Differential binding constants  $K_a$  for the 1:1 complexes of pyridinium salts with various anions (Cl, Br, and I added as tetrabutylammonium salt). The binding constants were determined by <sup>1</sup>H/<sup>19</sup>F NMR spectrometric analyses in CDCl<sub>3</sub>. Errors are estimated to be lower than 20%.

	Cl	Br	I
H <sub>benzyl</sub>	704	518	325
F <sub>ortho</sub>	388	352	236

Assuming 1:1 complexes, the association constants vary from 236 to 704, whereby they decrease in the series from chloride to bromide to iodide. A comparison of the binding constants determined by monitoring the benzylic proton signal with those by monitoring the *ortho*-fluorine signal reveals a significant difference. Moreover, the binding constants obtained from the *ortho*-fluorine signals are closer together than those for the benzyl protons. However, owing to the direct interaction of the anion with the electron-deficient C<sub>6</sub>F<sub>5</sub> unit, the results derived from the fluorine signal should be more expressive in anion- $\pi$  studies. Nevertheless, it is difficult to determine the role of anion- $\pi$  interactions in solution from the observed results.

## Conclusions

We observed anion– $\pi$  interactions in the solid-state structures of *N*-(pentafluorobenzyl)pyridinium salts. Thereby, the C<sub>6</sub>F<sub>5</sub> unit as well as the pyridinium group is involved in anion– $\pi$  contacts. In most solid-state structures, the anion is embedded in a number of CH–anion and anion– $\pi$  contacts. However, only the crystal structures of **1b-I<sub>3</sub>** and **1d** show a cooperative anion– $\pi$  interaction between the two electron-deficient arenes and the anion located between them. The most remarkable structure is the triiodide **1b-I<sub>3</sub>**, which encapsulates the anion in an electron-deficient channel. As this structure was observed by serendipity, future studies will focus on the trapping of polyhalides in electron-deficient cavities (e.g., to stabilize labile anionic species such as the tetraiodide dianion).

Although the performed NMR spectroscopic measurements do not give distinct evidence of the interactions of anions with electron-deficient arenes, the present study reveals that the calculated association constants strongly depend on the signal monitored during the analysis. This observation raises the question of whether the differences are related to the observation of different binding events. Further studies should reveal which signals are the most reliable for the investigation of weak forces such as anion– $\pi$  interactions in solution by NMR spectroscopy.

## Experimental Section

**General:** Solvents were used after distillation, and commercially available reagents were used as received without further purification. The <sup>1</sup>H and <sup>19</sup>F NMR spectroscopic data were measured with a Varian Mercury 300 or an Inova 400 spectrometer with samples in deuterated solvents. Mass spectra were recorded with a Finnigan SSQ 7000 or Thermo Deca XP spectrometer by using EI (70 eV) or ESI techniques. Infrared spectra were obtained with a Perkin–Elmer FTIR spectrometer. The samples were measured in KBr (4000–650 cm<sup>-1</sup>). Elemental analysis was performed with a CHN-O-Rapid Vario EL instrument from Heraeus. The melting points were obtained by using a Büchi B-540 instrument. Single-crystal X-ray data were collected at 123(2) K by using a Bruker-Nonius KappaCCD diffractometer with an APEX-II detector and graphite-monochromated Mo-K $\alpha$  ( $\lambda$  = 0.71073 Å) radiation. The COLLECT<sup>[17]</sup> software was used for the data collection ( $\theta$  and  $\omega$  scans), and DENZO-SMN<sup>[18]</sup> was used for the processing. The structures were solved by direct methods with SIR2004<sup>[19]</sup> and refined by full-matrix least-squares methods with the WinGX software,<sup>[20]</sup> which utilizes the SHELXL-97 module.<sup>[21]</sup> Lorentzian polarization and multiscan absorption corrections (SADABS)<sup>[22]</sup> were applied to all data. All C–H hydrogen atom positions were calculated and refined as riding atoms with 1.2 times the thermal parameters of the C atoms. H atoms from water molecules in **1a** were found from the electron-density map and restrained (by DFIX;  $s$  = 0.02) to a distance of 0.84 Å from the O atom with thermal parameters 1.5 times that of the O atom. CCDC-936265 (for **1a-H<sub>2</sub>O**), -936266 (for **1b-I<sub>3</sub>**), -936267 (for **1b**), -936268 (for **1c**), and -936269 (for **1d**) contain the supplementary crystallographic data for this paper. These data can be obtained free of charge from The Cambridge Crystallographic Data Centre via [www.ccdc.cam.ac.uk/data\\_request/cif](http://www.ccdc.cam.ac.uk/data_request/cif).

***N*-(Pentafluorobenzyl)pyridinium Bromide and Iodide (1a and 1b) and 4-*tert*-Butyl-*N*-(pentafluorobenzyl)pyridinium Bromide (2a):** The

synthesis of the *N*-(pentafluorobenzyl)pyridinium halides was performed neat; therefore, equimolar amounts of pyridine or 4-*tert*-butylpyridine were mixed together with the corresponding pentafluorobenzyl halide (bromide or iodide) at 50 °C, and the mixture was stirred until a colorless solid was obtained. The resulting solids were ground and dried under vacuum to remove the excesses starting materials.

**1a:** Light yellow solid; yield 1.30 g (3.8 mmol, quant.). M.p. 169 °C. <sup>1</sup>H NMR (MeOD, 300 MHz):  $\delta$  = 9.06 (br. d,  $J$  = 5.5 Hz, 2 H, H<sub>pyr</sub>), 8.68 (tt,  $J$  = 7.9, 1.3 Hz, 1 H, H<sub>pyr</sub>), 8.18 (m, 2 H, H<sub>pyr</sub>), 6.10 (s, 2 H, H<sub>benzyl</sub>) ppm. <sup>19</sup>F NMR (MeOD, 300 MHz):  $\delta$  = -142.68 (m, 2 F, F<sub>o</sub>), -153.10 (m, 1 F, F<sub>p</sub>), -163.21 (m, 2 F, F<sub>m</sub>) ppm. MS (ESI):  $m/z$  (%) = 260.1 (70) [M]<sup>+</sup>, 598.9 (100) [M<sub>2</sub>Br]<sup>+</sup>. IR (KBr):  $\tilde{\nu}$  = 3122 (w), 3019 (w), 2954 (w), 1875 (w), 2733 (w), 2384 (w), 2172 (w), 2084 (w), 1860 (w), 1662 (w), 1629 (m), 1579 (w), 1513 (vs), 1481 (s), 1436 (m), 1378 (w), 1308 (m), 1278 (w), 1211 (m), 1164 (m), 1128 (m), 1107 (m), 1083 (w), 1030 (s), 969 (s), 926 (s), 826 (w), 775 (m), 746 (w), 727 (m), 687 (s) cm<sup>-1</sup>. C<sub>12</sub>H<sub>7</sub>BrF<sub>5</sub>N (338.97): calcd. C 42.38, H 2.07, N 4.12; found C 42.37, H 2.09, N 4.16.

**1b:** Yellow solid; yield 300 mg (0.8 mmol, 80%). M.p. 200 °C. <sup>1</sup>H NMR (MeOD, 300 MHz):  $\delta$  = 9.09 (br. d,  $J$  = 5.7 Hz, 2 H, H<sub>pyr</sub>), 8.69 (tt,  $J$  = 7.8, 1.5 Hz, 1 H, H<sub>pyr</sub>), 8.19 (m, 2 H, H<sub>pyr</sub>), 6.11 (s, 2 H, H<sub>benzyl</sub>) ppm. <sup>19</sup>F NMR (MeOD, 300 MHz):  $\delta$  = -142.53 (m, 2 F, F<sub>o</sub>), -153.09 (m, 1 F, F<sub>p</sub>), -163.14 (m, 2 F, F<sub>m</sub>) ppm. MS (ESI):  $m/z$  (%) = 260.8 (100) [M]<sup>+</sup>, 181.3 (97) C<sub>7</sub>H<sub>2</sub>F<sub>5</sub><sup>+</sup>. IR (KBr):  $\tilde{\nu}$  = 3123 (w), 3047 (m), 3021 (w), 2956 (m), 2873 (w), 2375 (w), 2082 (w), 1991 (w), 1849 (w), 1751 (w), 1662 (w), 1629 (m), 1579 (w), 1512 (vs), 1481 (vs), 1435 (m), 1371 (m), 1306 (m), 1277 (w), 1211 (m), 1162 (m), 1127 (s), 1104 (m), 1079 (w), 1055 (w), 1027 (s), 968 (s), 924 (s), 864 (w), 827 (w), 772 (m), 745 (w), 723 (m), 683 (vs) cm<sup>-1</sup>. C<sub>12</sub>H<sub>7</sub>F<sub>5</sub>N (386.95): calcd. C 37.23, H 1.82, N 3.62; found C 37.03, H 1.77, N 3.55.

**2a:** White solid; yield 300 mg (0.8 mmol, 98%). M.p. 192 °C. <sup>1</sup>H NMR (CDCl<sub>3</sub>, 300 MHz):  $\delta$  = 9.57 (d,  $J$  = 6.8 Hz, 2 H, H<sub>pyr</sub>), 8.08 (d,  $J$  = 6.8 Hz, 2 H, H<sub>pyr</sub>), 6.56 (s, 2 H, H<sub>benzyl</sub>), 1.42 (s, 3 H, CH<sub>3</sub>) ppm. <sup>19</sup>F NMR (CDCl<sub>3</sub>, 300 MHz):  $\delta$  = -139.07 (m, 2 F, F<sub>o</sub>), -148.99 (m, 1 F, F<sub>p</sub>), -158.95 (m, 2 F, F<sub>m</sub>) ppm. MS (EI, 70 eV):  $m/z$  (%) = 316.1 (34) [M]<sup>+</sup>. IR (KBr):  $\tilde{\nu}$  = 3125 (w), 2941 (m), 2877 (w), 2709 (w), 2380 (w), 1986 (w), 1848 (w), 1641 (m), 1561 (w), 1507 (vs), 1472 (s), 1387 (m), 1304 (w), 1275 (w), 1241 (w), 1187 (m), 1126 (s), 1025 (s), 967 (s), 936 (s), 841 (m), 767 (w), 714 (w), 669 (m) cm<sup>-1</sup>. C<sub>16</sub>H<sub>15</sub>BrF<sub>5</sub>N (396.19): calcd. C 48.50, H 3.82, N 3.54; found C 48.62, H 3.63, N 3.51.

***N*-(Pentafluorobenzyl)pyridinium Tetrafluoroborate and Hexafluorophosphate (1c and 1d) and 4-*tert*-Butyl-*N*-(pentafluorobenzyl)pyridinium Tetrafluoroborate (2b):** The salts **1c**, **1d**, and **2b** were prepared by salt metathesis by using saturated aqueous solutions of *N*-(pentafluorobenzyl)pyridinium bromide (**1a**) or 4-*tert*-butyl-*N*-(pentafluorobenzyl)pyridinium bromide (**2a**). To these solutions, a saturated solution of the corresponding ammonium salt (tetrafluoroborate or hexafluorophosphate) was added. The precipitated solid was collected by filtration and dried in vacuo.

**1c:** White solid; yield 90 mg (0.3 mmol, 90%). M.p. 166 °C. <sup>1</sup>H NMR (MeOD, 300 MHz):  $\delta$  = 9.04 (br. d, 2 H, H<sub>pyr</sub>), 8.68 (tt,  $J$  = 7.8, 1.2 Hz, 1 H, H<sub>pyr</sub>), 8.16 (m, 2 H, H<sub>pyr</sub>), 6.07 (s, 2 H, H<sub>benzyl</sub>) ppm. <sup>19</sup>F NMR (MeOD, 300 MHz):  $\delta$  = -142.83 (m, 2 F, F<sub>o</sub>), -153.14 (m, 1 F, F<sub>p</sub>), -154.79 (s, 4 F), -163.29 (m, 2 F, F<sub>m</sub>) ppm. MS (EI, 70 eV):  $m/z$  (%) = 260.5 (100) [M]<sup>+</sup>, 181.1 (98) C<sub>7</sub>H<sub>2</sub>F<sub>5</sub><sup>+</sup>. IR (KBr):  $\tilde{\nu}$  = 3139 (w), 3097 (w), 3032 (w), 2324 (w), 2089 (w), 1663 (w), 1633 (w), 1516 (vs), 1487 (s), 1460 (w), 1439 (w), 1376 (w), 1308 (w), 1289 (w), 1220 (m), 1175 (m), 1130 (m), 1038 (vs,

br), 969 (s), 925 (s), 869 (w), 829 (w), 779 (m), 748 (w), 726 (w), 687 (s)  $\text{cm}^{-1}$ .  $\text{C}_{12}\text{H}_7\text{BF}_5\text{F}_4\text{N}$  (347.05): calcd. C 41.54, H 2.03, N 4.04; found C 41.18, H 1.71, N 4.09.

**1d**: White solid; yield 110 mg (0.3 mmol, 91%). M.p. 179 °C.  $^1\text{H}$  NMR ( $[\text{D}_6]\text{DMSO}$ , 300 MHz):  $\delta$  = 9.06 (br. d,  $J$  = 5.7 Hz, 2 H,  $\text{H}_{\text{pyr}}$ ), 8.65 (tt,  $J$  = 7.8, 1.5 Hz, 1 H,  $\text{H}_{\text{pyr}}$ ), 8.17 (m, 2 H,  $\text{H}_{\text{pyr}}$ ), 6.07 (s, 2 H,  $\text{H}_{\text{benzyl}}$ ) ppm.  $^{19}\text{F}$  NMR ( $[\text{D}_6]\text{DMSO}$ , 300 MHz):  $\delta$  = -70.19 (d,  $J$  = 710.6 Hz,  $\text{PF}_6$ ), -140.17 (m, 2 F,  $\text{F}_o$ ), -151.99 (m, 1 F,  $\text{F}_p$ ), -161.50 (m, 2 F,  $\text{F}_m$ ) ppm. MS (EI, 70 eV):  $m/z$  (%) = 260.1 (100)  $[\text{M}]^+$ , 181.1 (89)  $\text{C}_7\text{H}_5\text{F}_5^+$ . IR (KBr):  $\tilde{\nu}$  = 3145 (w), 3102 (w), 1659 (w), 1627 (w), 1511 (m), 1451 (w), 1396 (w), 1357 (w), 1310 (w), 1278 (w), 1226 (w), 1176 (w), 1130 (m), 1112 (w), 1026 (m), 970 (m), 917 (m), 878 (w), 824 (vs), 778 (m), 738 (m), 690 (m)  $\text{cm}^{-1}$ .  $\text{C}_{12}\text{H}_7\text{F}_5\text{F}_6\text{NP}$  (405.01): calcd. C 35.57, H 35.41, N 3.46; found C 35.41, H 1.92, N 3.48.

**2b**: White solid; yield 86 mg (0.2 mmol, 85%). M.p. 150 °C.  $^1\text{H}$  NMR ( $\text{CDCl}_3$ , 400 MHz):  $\delta$  = 8.77 (d,  $J$  = 7.0 Hz, 2 H,  $\text{H}_{\text{pyr}}$ ), 8.00 (d,  $J$  = 7.0 Hz, 2 H,  $\text{H}_{\text{pyr}}$ ), 5.96 (s, 2 H,  $\text{H}_{\text{benzyl}}$ ), 1.41 (s, 3 H,  $\text{CH}_3$ ) ppm.  $^{19}\text{F}$  NMR ( $\text{CDCl}_3$ , 400 MHz):  $\delta$  = -140.22 (m, 2 F,  $\text{F}_o$ ), -148.67 (m, 1 F,  $\text{F}_p$ ), -152.38 (s, 4 F,  $\text{BF}_4$ ), -158.95 (m, 2 F,  $\text{F}_m$ ) ppm. MS (EI, 70 eV):  $m/z$  (%) = 316.1 (34)  $[\text{M}]^+$ . IR (KBr):  $\tilde{\nu}$  = 3327 (w), 3146 (w), 3083 (w), 2972 (w), 2088 (w), 1980 (w), 1646 (m), 1572 (w), 1509 (vs), 1471 (m), 1364 (w), 1305 (w), 1280 (w), 1183 (w), 1120 (m), 1034 (vs), 964 (m), 916 (m), 817 (w), 762 (w), 734 (w), 693 (w), 657 (w)  $\text{cm}^{-1}$ .  $\text{C}_{16}\text{H}_{15}\text{BF}_5\text{F}_4\text{N}$  (403.09): calcd. C 47.67, H 3.75, N 3.47; found C 47.58, H 3.74, N 4.33.

### Crystal Data

**1a**: Colorless prisms from  $\text{DMSO}/\text{EtOAc}$ ,  $\text{C}_{12}\text{H}_9\text{BrF}_5\text{NO}$  (358.11), crystal size  $0.23 \times 0.20 \times 0.09$  mm, monoclinic, space group  $P2_1/c$  (no. 14),  $a$  = 15.5655(4),  $b$  = 6.9581(2),  $c$  = 11.7428(3) Å,  $\beta$  = 92.159(2)°,  $V$  = 1270.92(6) Å<sup>3</sup>,  $Z$  = 4,  $D_{\text{calcd.}}$  = 1.872  $\text{Mg m}^{-3}$ ,  $\mu$  = 3.290  $\text{mm}^{-1}$ ,  $F(000)$  = 704, 7151 collected reflections ( $\theta_{\text{max}}$  = 25.02°) of which 2236 independent ( $R_{\text{int}}$  = 0.0326) and 1889 with  $I > 2\sigma(I)$ ,  $T_{\text{max}}$  = 0.7561,  $T_{\text{min}}$  = 0.5183, full-matrix least squares on  $F^2$  with two restraints and 187 parameters, GOF = 1.047,  $R1$  = 0.0243 [ $I > 2\sigma(I)$ ],  $wR2$  (all data) = 0.0513, largest peak/hole = 0.296/-0.293  $\text{e}^{-\text{Å}^{-3}}$ .

**1b**: Colorless plates from  $\text{DMF}/\text{Et}_2\text{O}$ ,  $\text{C}_{12}\text{H}_7\text{F}_5\text{IN}$  (387.09), crystal size  $0.30 \times 0.16 \times 0.06$  mm, triclinic, space group  $P\bar{1}$  (no. 2),  $a$  = 9.4367(2),  $b$  = 11.6827(2),  $c$  = 12.6011(3) Å,  $\alpha$  = 103.4940(10),  $\beta$  = 104.5680(10),  $\gamma$  = 97.3260(10)°,  $V$  = 1281.59(5) Å<sup>3</sup>,  $Z$  = 4 ( $Z'$  = 2),  $D_{\text{calcd.}}$  = 2.006  $\text{Mg m}^{-3}$ ,  $\mu$  = 2.544  $\text{mm}^{-1}$ ,  $F(000)$  = 736, 7612 collected reflections ( $\theta_{\text{max}}$  = 25.02°) of which 4500 independent ( $R_{\text{int}}$  = 0.0167) and 4028 with  $I > 2\sigma(I)$ ,  $T_{\text{max}}$  = 0.8624,  $T_{\text{min}}$  = 0.5158, full-matrix least squares on  $F^2$  with 0 restraints and 343 parameters, GOF = 1.063,  $R1$  = 0.0204 [ $I > 2\sigma(I)$ ],  $wR2$  (all data) = 0.0469, largest peak/hole = 0.315/-0.482  $\text{e}^{-\text{Å}^{-3}}$ .

**1b-I<sub>3</sub>**: Red plates from  $\text{MeOH}$ ,  $\text{C}_{12}\text{H}_7\text{F}_5\text{I}_3\text{N}$  (640.89), crystal size  $0.13 \times 0.12 \times 0.07$  mm, triclinic, space group  $P\bar{1}$  (no. 2),  $a$  = 9.2487(2),  $b$  = 9.3202(2),  $c$  = 10.4842(3) Å,  $\alpha$  = 98.063(2),  $\beta$  = 111.3060(10),  $\gamma$  = 90.182(2)°,  $V$  = 832.21(3) Å<sup>3</sup>,  $Z$  = 2,  $D_{\text{calcd.}}$  = 2.558  $\text{Mg m}^{-3}$ ,  $\mu$  = 5.674  $\text{mm}^{-1}$ ,  $F(000)$  = 580, 4989 collected reflections ( $\theta_{\text{max}}$  = 25.25°) of which 2981 independent ( $R_{\text{int}}$  = 0.0159) and 2763 with  $I > 2\sigma(I)$ ,  $T_{\text{max}}$  = 0.6922,  $T_{\text{min}}$  = 0.5258, full-matrix least squares on  $F^2$  with 0 restraints and 193 parameters, GOF = 1.134,  $R1$  = 0.0212 [ $I > 2\sigma(I)$ ],  $wR2$  (all data) = 0.0499, largest peak/hole = 0.450/-0.498  $\text{e}^{-\text{Å}^{-3}}$ .

**1c**: Colorless plates from  $\text{MeOH}/\text{EtOAc}$ ,  $\text{C}_{12}\text{H}_7\text{BF}_9\text{N}$  (347.00), crystal size  $0.25 \times 0.15 \times 0.08$  mm, triclinic, space group  $P\bar{1}$  (no. 2),  $a$  = 9.2900(2),  $b$  = 11.8365(3),  $c$  = 12.7478(3) Å,  $\alpha$  = 104.0380(10),  $\beta$  = 103.722(2),  $\gamma$  = 97.238(2)°,  $V$  = 1295.79(5) Å<sup>3</sup>,  $Z$  = 4 ( $Z'$  = 2),

$D_{\text{calcd.}}$  = 1.779  $\text{Mg m}^{-3}$ ,  $\mu$  = 0.195  $\text{mm}^{-1}$ ,  $F(000)$  = 688, 7818 collected reflections ( $\theta_{\text{max}}$  = 25.25°) of which 4672 independent ( $R_{\text{int}}$  = 0.0250) and 3463 with  $I > 2\sigma(I)$ ,  $T_{\text{max}}$  = 0.9846,  $T_{\text{min}}$  = 0.9528, full-matrix least squares on  $F^2$  with 0 restraints and 415 parameters, GOF = 1.030,  $R1$  = 0.0417 [ $I > 2\sigma(I)$ ],  $wR2$  (all data) = 0.0941, largest peak/hole = 0.283/-0.240  $\text{e}^{-\text{Å}^{-3}}$ .

**1d**: Colorless blocks from  $\text{DMF}/\text{Et}_2\text{O}$ ,  $\text{C}_{12}\text{H}_7\text{F}_{11}\text{NP}$  (405.16), crystal size  $0.30 \times 0.25 \times 0.20$  mm, orthorhombic, space group  $Pbca$  (no. 61),  $a$  = 6.84290(10),  $b$  = 12.6254(2),  $c$  = 31.8647(4) Å,  $V$  = 2752.93(7) Å<sup>3</sup>,  $Z$  = 8,  $D_{\text{calcd.}}$  = 1.955  $\text{Mg m}^{-3}$ ,  $\mu$  = 0.331  $\text{mm}^{-1}$ ,  $F(000)$  = 1600, 4557 collected reflections ( $\theta_{\text{max}}$  = 25.25°) of which 2475 independent ( $R_{\text{int}}$  = 0.0136) and 2150 with  $I > 2\sigma(I)$ ,  $T_{\text{max}}$  = 0.9368,  $T_{\text{min}}$  = 0.9073, full-matrix least squares on  $F^2$  with 0 restraints and 226 parameters, GOF = 1.029,  $R1$  = 0.0330 [ $I > 2\sigma(I)$ ],  $wR2$  (all data) = 0.0792, largest peak/hole = 0.287/-0.302  $\text{e}^{-\text{Å}^{-3}}$ .

**Supporting Information** (see footnote on the first page of this article): Crystal stacking in **1b**, anion- $\pi$  distances in the previously described structures, data for titration experiments,  $^1\text{H}$  and  $^{19}\text{F}$  NMR spectra.

### Acknowledgments

This work was supported by the Fonds der Chemischen Industrie (M. A.) and the Academy of Finland (K. R.: project nos 122350, 140718, 265328, and 263256).

- [1] E. M. Wright, J. M. Diamond, *Physiol. Rev.* **1977**, *57*, 109–156.
- [2] P. Bauduin, A. Renocourt, D. Touraud, W. Kunz, B. W. Ninham, *Curr. Opin. Colloid Interface Sci.* **2004**, *9*, 43–47.
- [3] F. M. Ashcroft, *Ion Channels and Disease*, Academic Press, San Diego, **2000**.
- [4] P. D. Beer, P. A. Gale, *Angew. Chem.* **2001**, *113*, 502–532; *Angew. Chem. Int. Ed.* **2001**, *40*, 486–516.
- [5] a) P. Ballester, *Struct. Bonding (Berlin)* **2008**, *129*, 127–174; b) B. L. Schottel, H. T. Chifotides, K. R. Dunbar, *Chem. Soc. Rev.* **2008**, *37*, 68–83; c) B. P. Hay, V. S. Bryantsev, *Chem. Commun.* **2008**, *21*, 2417–2428; d) P. Gamez, T. J. Mooibroek, S. J. Teat, J. Reedijk, *Acc. Chem. Res.* **2007**, *40*, 435–444; e) A. Robertazzi, F. Krull, E.-W. Knapp, P. Gamez, *CrystEngComm* **2011**, *13*, 3293–3300; f) A. Frontera, P. Gamez, M. Mascal, T. J. Mooibroek, J. Reedijk, *Angew. Chem.* **2011**, *123*, 9736–9756; *Angew. Chem. Int. Ed.* **2011**, *50*, 9564–9583.
- [6] H.-J. Schneider, F. Werner, T. Blatter, *J. Phys. Org. Chem.* **1993**, *6*, 590–594.
- [7] a) I. Alkorta, I. Rozas, J. Elguero, *J. Am. Chem. Soc.* **2002**, *124*, 8593–8598; b) M. Mascal, A. Armstrong, M. D. Bartberger, *J. Am. Chem. Soc.* **2002**, *124*, 6274–6276; c) A. Frontera, F. Saczewski, M. Gdaniec, E. Dziemidowicz-Borys, A. Kurland, P. M. Deya, D. Quinonero, C. Garau, *Chem. Eur. J.* **2005**, *11*, 6560–6567; d) C. Garau, D. Quinonero, A. Frontera, P. Ballester, A. Costa, P. M. Deya, *J. Phys. Chem. A* **2005**, *109*, 9632–4637; e) D. Quinonero, C. Garau, A. Frontera, P. Ballester, A. Costa, P. M. Deya, *Chem. Phys. Lett.* **2002**, *359*, 486–492; f) C. Garau, A. Frontera, D. Quinonero, P. Ballester, A. Costa, P. M. Deya, *J. Phys. Chem. A* **2004**, *108*, 9423–9427; g) C. Garau, A. Frontera, P. Ballester, D. Quinonero, A. Costa, P. M. Deya, *Eur. J. Org. Chem.* **2005**, 179–183.
- [8] For example: a) P. Ballester, *Acc. Chem. Res.* **2013**, *46*, 874–884; b) S. Li, S.-X. Fa, Q.-Q. Wang, D.-X. Wang, M.-X. Wang, *J. Org. Chem.* **2012**, *77*, 1860–1867; c) M. Giese, M. Albrecht, T. Krappitz, M. Peters, V. Gossen, G. Raabe, A. Valkonen, K. Rissanen, *Chem. Commun.* **2012**, *48*, 9983–9985; d) D. X. Wang, Q. Q. Wang, Y. C. Han, Y. L. Wang, Z. T. Huang, M. X. Wang, *Chem. Eur. J.* **2010**, *16*, 13053–13057; e) S. Guha, S. Saha, *J. Am. Chem. Soc.* **2010**, *132*, 17674–17677; f) D. X. Wang, Q. Y. Zheng, Q. Q. Wang, M. X. Wang, *Angew. Chem.*

- 2008, 120, 7595; *Angew. Chem. Int. Ed.* **2008**, 47, 7485–7488; g) H. Maeda, A. Osuka, H. Furuta, *J. Inclusion Phenom. Macrocyclic Chem.* **2004**, 49, 33–36; h) H. Maeda, H. Furuta, *J. Porphyrins Phthalocyanines* **2004**, 8, 67–76; i) Y. S. Rosokha, S. V. Lindeman, S. V. Rosokha, J. K. Kochi, *Angew. Chem.* **2004**, 116, 4750–4752; *Angew. Chem. Int. Ed.* **2004**, 43, 4650–4652; j) O. B. Berryman, F. Hof, M. J. Hynes, D. W. Johnson, *Chem. Commun.* **2006**, 506–508; k) M. Staffilani, K. S. B. Hancock, J. W. Steed, K. T. Holman, J. L. Atwood, R. K. Juneja, R. S. Burkhalter, *J. Am. Chem. Soc.* **1997**, 119, 6324–6335; l) R. M. Fairchild, K. T. Holman, *J. Am. Chem. Soc.* **2005**, 127, 16364–16365.
- [9] M. Albrecht, C. Wessel, M. de Groot, K. Rissanen, A. Lüchow, *J. Am. Chem. Soc.* **2008**, 130, 4600–4601.
- [10] M. Albrecht, M. Müller, O. Mergel, A. Valkonen, K. Rissanen, *Chem. Eur. J.* **2010**, 16, 5062–5069.
- [11] M. Giese, M. Albrecht, C. Banwarth, G. Raabe, A. Valkonen, K. Rissanen, *Chem. Commun.* **2011**, 47, 8542–8544.
- [12] M. Giese, M. Albrecht, G. Ivanova, A. Valkonen, K. Rissanen, *Supramol. Chem.* **2012**, 24, 48–55.
- [13] M. Müller, M. Albrecht, V. Gossen, T. Peters, A. Hoffmann, G. Raabe, A. Valkonen, K. Rissanen, *Chem. Eur. J.* **2010**, 16, 12446–12453.
- [14] M. Müller, M. Albrecht, J. Sackmann, A. Hoffmann, F. Dierkes, A. Valkonen, K. Rissanen, *Dalton Trans.* **2010**, 39, 11329–11334.
- [15] a) Y. Zheng, Y.-Q. Peng, M.-H. Feng, S. Han, J.-R. Zhou, X.-P. Liu, L.-M. Yang, C.-L. Ni, *Synth. React. Inorg. Met.-Org. Nano-Met. Chem.* **2011**, 41, 839–844; b) E. Anders, J. G. Tropsch, E. Irmer, G. M. Sheldrick, *Chem. Ber.* **1990**, 123, 321–325.
- [16] a) K. A. Connors, *Binding Constants*, Wiley, New York, **1987**; b) C. S. Wilcox in *Frontiers in Supramolecular Chemistry and Photochemistry* (Eds.: H.-J. Schneider, H. Dürr), Wiley-VCH, Weinheim, **1991**, p. 123.
- [17] COLLECT, Bruker AXS, Inc., Madison, **2008**.
- [18] Z. Otwinowski, W. Minor in *Methods in Enzymology*, volume 276 (“Macromolecular Crystallography”, Part A) (Eds.: C. W. Carter Jr., R. M. Sweet), Elsevier, USA, **1997**, pp. 307–326.
- [19] M. C. Burla, R. Caliandro, M. Camalli, B. Carrozzini, G. L. Casciaro, L. De Caro, C. Giacovazzo, G. Polidori, R. Spagna, *J. Appl. Crystallogr.* **2005**, 38, 381–388.
- [20] L. J. Farrugia, *J. Appl. Crystallogr.* **1999**, 32, 837–838.
- [21] G. M. Sheldrick, *Acta Crystallogr., Sect. A: Found. Crystallogr.* **2008**, 64, 112–122.
- [22] G. M. Sheldrick, *SADABS*, University of Göttingen, **1996**.

Received: September 3, 2013  
Published Online: January 17, 2014